

Strain and friction induced by van der Waals interaction in individual single walled carbon nanotubes

Cite as: Appl. Phys. Lett. **90**, 253113 (2007); <https://doi.org/10.1063/1.2749870>

Submitted: 31 January 2007 . Accepted: 28 May 2007 . Published Online: 21 June 2007

Hyungbin Son, Georgii G. Samsonidze, Jing Kong, Yingying Zhang, Xiaojie Duan, Jin Zhang, Zhongfan Liu, and Mildred S. Dresselhaus



View Online



Export Citation

ARTICLES YOU MAY BE INTERESTED IN

[Mechanical stress relaxation in adhesively clamped carbon nanotube resonators](#)

AIP Advances **8**, 025118 (2018); <https://doi.org/10.1063/1.5020704>

[Making graphene visible](#)

Applied Physics Letters **91**, 063124 (2007); <https://doi.org/10.1063/1.2768624>

[Raman Spectrum of Graphite](#)

The Journal of Chemical Physics **53**, 1126 (1970); <https://doi.org/10.1063/1.1674108>

Lock-in Amplifiers
up to 600 MHz



Strain and friction induced by van der Waals interaction in individual single walled carbon nanotubes

Hyungbin Son, Georgii G. Samsonidze, and Jing Kong^{a)}

Department of Electrical Engineering and Computer Science, Massachusetts Institute of Technology, Cambridge, Massachusetts 02139-4307

Yingying Zhang, Xiaojie Duan, Jin Zhang, and Zhongfan Liu

Centre for Nanoscale Science and Technology, Key Laboratory for the Physics and Chemistry of Nanodevices, College of Chemistry and Molecular Engineering, Peking University, Beijing 100871, People's Republic of China

Mildred S. Dresselhaus

Department of Electrical Engineering and Computer Science and Department of Physics, Massachusetts Institute of Technology, Cambridge, Massachusetts 02139-4307

(Received 31 January 2007; accepted 28 May 2007; published online 21 June 2007)

Axial strain is introduced into individual single wall carbon nanotubes (SWCNTs) suspended from a trench-containing Si/SiO₂ substrate by employing the van der Waals interaction between the SWCNT and the substrate. Resonance Raman spectroscopy is used to characterize the strain, and up to 3% axial strain is observed. It is also found that a significant friction between the SWCNT and the substrate, on the order of 10 pN/nm, governs the localization and propagation of the strain in the SWCNTs sitting on the substrate. This method can be applied to introduce strain into materials sitting on a substrate, such as a graphene sheet. © 2007 American Institute of Physics.

[DOI: 10.1063/1.2749870]

Due to their remarkable electronic and optical properties, single wall carbon nanotubes (SWCNTs) have been under intensive investigation.¹ Being a one dimensional system, it is predicted that strain can dramatically modify the electronic and optical properties of SWCNTs.² Thus, strain is envisioned as a method for tuning the electronic and optical properties of SWCNTs for device applications.^{2,3} However, most of the investigations have relied on manual manipulations to introduce strains in the SWCNTs.^{4,5} In this work, we report an alternative way of producing strain in many individual SWCNTs simultaneously by employing the van der Waals (vdW) interactions between the nanotube and the substrate. Resonance Raman spectroscopy (RRS) is used to confirm and characterize the strain in the SWCNTs. Our study suggests a possible method for introducing strain into SWCNT devices on a large scale.

We start the discussion by presenting a simple model for how strain is generated by the vdW interaction in SWCNTs bound to a substrate. Line ABC in Figure 1 shows a molecular wire contacting a substrate with an angle α . Assume that the wire is inelastic so that we can exclude elastic energy for simplicity. If the wire in the initial form (ABC) is pulled from one end (point A) to the final form ($A'B'C$) while keeping the contact angle α constant, the work done in this process must be equal to the change in the total binding energy,

$$T(1 - \cos \alpha)dx = E_B dx, \tag{1}$$

where E_B is the binding energy per unit length, dx is the length of BB' , and T is the tension of the wire. Thus,

$$T = E_B \frac{1}{1 - \cos \alpha}. \tag{2}$$

At a small angle α , T has a much larger value than E_B , thereby possibly introducing a large strain to the molecular wire. For SWCNTs on a H-passivated Si(100) surface, E_B is about 2–3 eV/nm for SWCNTs with 1–2 nm diameter.⁶ As long as the surface is not chemically active, E_B on a different surface is expected to be similar since the Hamaker constants for different materials are similar.⁷

To introduce strain in individual SWCNTs, we used a silicon substrate with 300 nm deep trenches with different widths: 1.5, 3, and 6 μm . The trenches were patterned on a 300 nm silicon oxide film by dry etching. Well-separated ultralong aligned SWCNTs were grown across the trenches using an ethanol chemical vapor deposition method at 900 °C.⁸ Figure 2(a) shows a scanning electron microscope (SEM) image of the SWCNTs grown on the substrate. Figure 2(b) is an atomic force microscope (AFM) image of a single SWCNT grown across the trenches (dark). From the AFM and SEM images, we found that the SWCNTs often touch

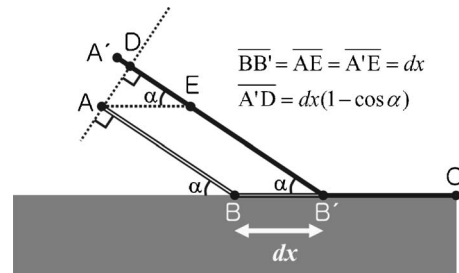


FIG. 1. Molecular wire making contact with a substrate at an angle α . The wire in the initial form (ABC) is pulled by a force T to the final form ($A'B'C$). The vdW binding energy E_B between the substrate and the wire can sustain the tension in the wire.

^{a)} Author to whom correspondence should be addressed; electronic mail: jingkong@mit.edu

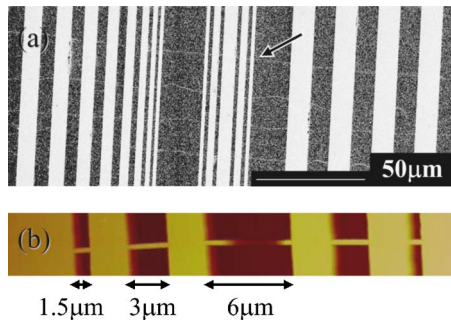


FIG. 2. (Color online) (a) SEM image of long aligned SWCNTs grown across trenches. The SWCNT described in Fig. 3 is indicated by the arrow. (b) AFM image of a SWCNT grown across the 1.5, 3, and 6 μm wide trenches. The SWCNT falls down to the bottom of the 6 μm wide trench.

the bottom of the 6 μm wide trenches [Fig. 2(b)] at a certain angle like in Fig. 1; therefore, it is expected that strain will develop in these SWCNTs.

RRS was employed to characterize the vibrational modes of the SWCNTs along their lengths. A micro-Raman setup in a backscattering geometry with a 50 \times objective (numerical aperture=0.8) is used for collecting spectra with laser excitation wavelengths of 514, 621, 633, and 647 nm. The laser spot size is about 1 μm^2 . Using an automated stage, Raman spectra are taken over the region near the trenches. Spectra are taken at two different laser power levels (0.9 and ~ 3 mW) to ensure there is no heating effect. By plotting the integrated peak intensity of a vibrational mode in a two-dimensional (2D) map, we can construct an image of the SWCNT. Figure 3(b) shows such an image constructed from the G band between 1500 and 1600 cm^{-1} , where the color bar shows the intensity scale. Figure 3(a) shows the intensity map of the silicon peak at 520 cm^{-1} taken in the same region, as Fig. 3(b), which identifies the trench regions. In Fig. 3(c), we plot the Raman spectra of the G band along the length of the SWCNT and the frequency of the most intense peak is marked by the red dashed line.⁹ A downshift in this frequency as y increases can be clearly seen. We observed five semiconducting SWCNTs (S-SWCNTs) with to-

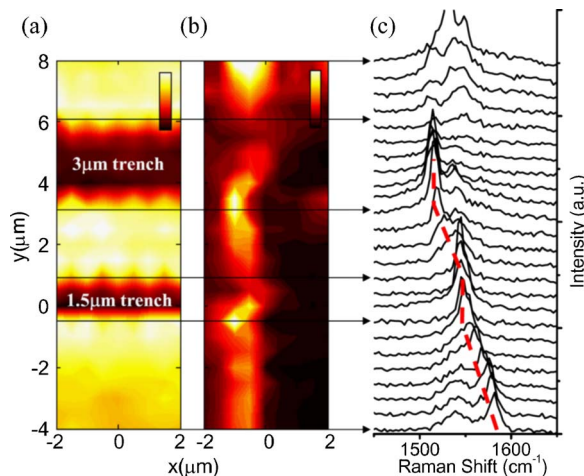


FIG. 3. (Color online) (a) 2D integrated intensity map of the silicon peak at 520 cm^{-1} . The dark regions correspond to the trench regions. (b) 2D integrated intensity map of the G band between 1500 and 1600 cm^{-1} taken from a SWCNT in the same region as in (a). (c) Actual G -band spectra along the length of the SWCNT shown in (b). The peak frequency of the most intense peak is observed to shift linearly with respect to the position on the substrate and remains constant across the trenches.

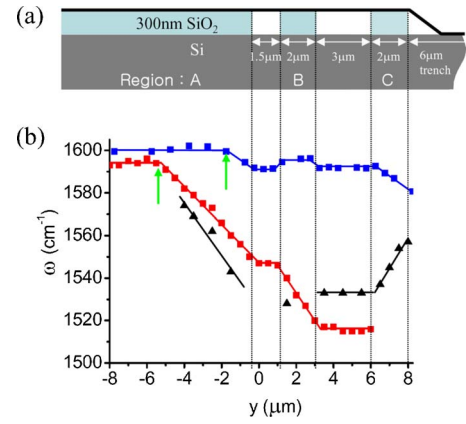


FIG. 4. (Color online) (a) Schematic of a SWCNT grown across the 1.5, 3, and 6 μm wide trenches. The SWCNT falls down the 6 μm trench in this example. (b) ω_{G^+} with respect to position y obtained from three SWCNTs (shown as black triangles, blue squares, and red diamonds) in the region shown in (a). The strain generated at $y=8$ μm propagates to the left until it completely relaxes at the points indicated by the green arrows due to the friction between the SWCNTs and the substrate.

tal frequency downshifts of 3–8 cm^{-1} and three other S-SWCNTs with total frequency downshifts of 20, 54, 80 cm^{-1} , and these latter three are shown as blue squares, black triangles, and red diamonds, respectively, in Fig. 4(b).¹⁰ The G -band frequency at positions far away from the trench region lies between 1590 and 1600 cm^{-1} . This corresponds to the frequency of the A -symmetry mode of the G^+ band (ω_{G^+}) in unstrained semiconducting SWCNTs.¹¹ It has been reported that ω_{G^+} downshifts linearly (28 $\text{cm}^{-1}/1\%$ axial strain) with respect to the axial strain of up to 1.6% strain in semiconducting SWCNTs.⁵

Using our model in Fig. 1, the observed frequency shift can be explained in the following: The axial strain is generated at the trench where the SWCNT falls down to the bottom and the strain propagates along the SWCNT due to the substrate-SWCNT friction until it relaxes to zero. With a classical elastic model, the propagation of strain can be expressed as

$$\frac{d\varepsilon}{dy} = \frac{d}{dy} \frac{T}{AY} = \frac{dT}{dy} \frac{1}{AY} = \frac{f}{AY}, \quad (3)$$

where ε is the axial strain and A is the cross sectional area of the SWCNTs, which is 0.34 nm times the circumference of the SWCNTs,¹² Y is Young's modulus for SWCNTs, which is 1 TPa,¹² and f is the friction per unit length of SWCNTs. The linear frequency shift behavior indicates that f is constant along the length of each SWCNT. We find that f is about 5 pN/nm for SWCNTs sitting on a SiO_2 substrate, which is about an order of magnitude higher per carbon atom than values reported for wall to wall interaction in double walled carbon nanotubes and multiwalled carbon nanotubes.^{13,14}

To verify that the vdW interaction is sufficient to induce the observed strain, we have estimated the strain using the previously reported E_B .⁶ From the SEM and AFM images, we measure the angle α for different SWCNTs, which ranges from about 8.5° to 30°. We calculate the strain based on the tension using Eq. (2),

$$\varepsilon = \frac{T}{AY} = \frac{E_B}{AY} \frac{1}{1 - \cos \alpha}. \quad (4)$$

The resulting strain ranges from a negligible value (less than 0.2%) to more than 3%, which is consistent with values observed in our study. Note that although the vdW interaction is universal, supporting such a large strain solely by the vdW interaction is possible only in structures with nanometer thickness. In a general ribbonlike structure, E_B is roughly proportional to the ribbon width (E_B is the energy per unit length), whereas the cross sectional area A is proportional to the ribbon width times the thickness of the structure. Thus, the strain is inversely proportional to the thickness of the structure.

The large variation of the strain observed in different individual SWCNTs is mostly due to variation in the contact angle α but not to variation in E_B . This is most likely due to randomness in the amount of slack in the SWCNTs. Therefore, a better engineered trench profile and an improved process of the SWCNTs falling down in a trench in a more controlled way would significantly reduce this randomness, making the method more useful for introducing a uniform strain on a large scale.

In conclusion, we have demonstrated a method to introduce strain into individual SWCNTs using a vdW interaction without manual manipulation. This method allows measurements of strain up to 3% and opens opportunities for further exploration of nonlinear effects under large strain. It will allow the generation of strains in devices on a large scale and in other interesting nanomaterials such as a graphene sheet.^{15,16}

H.S. and J.K. acknowledge the support of the Intel Higher Education Program and the MSD Focus Center, one of five research centers funded under the Focus Center Research Program and a Semiconductor Corporation program. G.G.S. and M.S.D. acknowledge the support from NSF under Grant No. DMR04-05538. Y.Z., X.D., J.Z. and Z.L. acknowledge the support from NSFC (90206023) and MOST (2001CB6105). This work was carried out using the Raman

facility in the Spectroscopy Laboratory supported by NSF CHE 0111370 and by NIH RR02594 grants.

- ¹P. L. McEuen, *Phys. World* **13**, 31 (2000).
- ²L. Yang and J. Han, *Phys. Rev. Lett.* **85**, 154 (2000).
- ³R. Hyed, A. Charlier, and E. McRae, *Phys. Rev. B* **55**, 6820 (1997).
- ⁴E. D. Minot, Y. Yaish, V. Sazonova, J.-Y. Park, M. Brink, and P. L. McEuen, *Phys. Rev. Lett.* **90**, 156401 (2003).
- ⁵S. B. Cronin, A. K. Swan, M. S. Ünlü, B. B. Goldberg, M. S. Dresselhaus, and M. Tinkham, *Phys. Rev. Lett.* **93**, 167401 (2004).
- ⁶T. Hertel, R. E. Walkup, and P. Avouris, *Phys. Rev. B* **58**, 13870 (1998).
- ⁷J. Israelachvili, *Intermolecular and Surface Forces* (Academic, London, 1994).
- ⁸L. X. Zheng, M. J. O'Connell, S. K. Doorn, X. Z. Liao, Y. H. Zhao, E. A. Akhador, M. A. Hoffbauer, B. J. Roop, Q. X. Jia, R. C. Dye, D. E. Peterson, S. M. Huang, J. Liu, and Y. T. Zhu, *Nat. Mater.* **3**, 673 (2004).
- ⁹For the SWNT in Fig. 3, we found two radial breathing mode (RBM) peaks at 128 and 173 cm^{-1} . In the plot of the RBM peak frequencies vs resonant transition energies based on the extended tight binding model (Ref. 17), RBM peaks at 128 and 173 cm^{-1} correspond to semiconducting and metallic SWCNTs, respectively. We conclude that this is a bundle of a semiconducting SWCNT and a metallic SWCNT. The broad peak at 1540 cm^{-1} , which shows a Breit-Wigner-Fano line shape, corresponds to the metallic SWCNT in the bundle (Ref. 18). We also see changes in the Raman intensity along the length of the SWCNTs [Fig. 3(c)]. This is expected due to the change in the electronic transition energies when the SWCNT is under strain (Refs. 2 and 3).
- ¹⁰The typical full width at half maximum linewidth of the *G* band is about 10 cm^{-1} and the typical peak accuracy of the *G* band is about $\pm 1 \text{ cm}^{-1}$.
- ¹¹A. Jorio, M. A. Pimenta, A. G. Souza Filho, Ge. G. Samsonidze, A. K. Swan, M. S. Ünlü, B. B. Goldberg, R. Saito, G. Dresselhaus, and M. S. Dresselhaus, *Phys. Rev. Lett.* **90**, 107403 (2004).
- ¹²J. P. Lu, *Phys. Rev. Lett.* **79**, 1297 (1997).
- ¹³Y. Zhao, C. C. Ma, G. Chen, and Q. Jiang, *Phys. Rev. Lett.* **91**, 175504 (2004).
- ¹⁴J. Cumings and A. Zettl, *Science* **289**, 602 (2000).
- ¹⁵K. S. Novoselov, A. K. Geim, S. V. Morozov, D. Jiang, M. I. Katsnelson, I. V. Grigorieva, S. V. Dubonos, and A. A. Firsov, *Nature (London)* **438**, 197 (2005).
- ¹⁶Y. Zhang, Y. W. Tan, H. L. Stormer, and Philip Kim, *Nature (London)* **438**, 201 (2005).
- ¹⁷Ge. G. Samsonidze, R. Saito, N. Kobayashi, A. Grüneis, J. Jiang, A. Jorio, S. G. Chou, G. Dresselhaus, and M. S. Dresselhaus, *Appl. Phys. Lett.* **85**, 5703 (2004).
- ¹⁸H. Kataura, Y. Kumazawa, Y. Maniwa, I. Umez, S. Suzuki, Y. Ohtsuka, and Y. Achiba, *Synth. Met.* **103**, 2555 (1999).